Determination of the pK_a Values of Active-Center Cysteines, Cysteines-32 and -35, in *Escherichia coli* Thioredoxin by Raman Spectroscopy†

Huimin Li,‡ Chad Hanson,§ James A. Fuchs,§ Clare Woodward,§ and George J. Thomas, Jr.*,‡

Division of Cell Biology and Biophysics, School of Biological Sciences, University of Missouri—Kansas City, Kansas City, Missouri 64110, and Department of Biochemistry, University of Minnesota, St. Paul, Minnesota 55108

Received November 17, 1992; Revised Manuscript Received March 10, 1993

ABSTRACT: We have determined the pK_a values for thiol–thiolate equilibria of *Escherichia coli* thioredoxin and compared structural properties of reduced and oxidized forms of the protein in solution by Raman spectroscopy. Ionization and hydrogen-bonding states of the two cysteine sulfhydryls (Cys32 and Cys35) in reduced thioredoxin were determined by monitoring the complex Raman SH stretching band (Li & Thomas, 1991) as a function of pH in the range 4.0 < pH < 12.2. The Raman SH markers indicate the following: (i) Both sulfhydryls of the native protein are relatively robust hydrogen-bond donors, but one is a stronger hydrogen-bond donor than the other. (ii) The sulfhydryl which donates the weaker hydrogen bond, assigned tentatively to Cys32, is preferentially titrated to the thiolate ion (S^-) as the solution pH is increased from 4 to 7. Water or a hydroxyl oxygen is the probable acceptor for the Cys32 S–H donor. (iii) The sulfhydryl which donates the stronger hydrogen bond, Cys35, resists substantial ionization until roughly 50% of the more acidic sulfhydryl has been titrated. A carbonyl oxygen is proposed as the likely acceptor of the Cys35 S–H donor. (iv) The Raman titration data indicate pK_1 = 7.1 ± 0.2 and pK_2 = 7.9 ± 0.2 for the two thiol–thiolate equilibria. The lower pK_a, which is the more strongly perturbed, is assigned tentatively to Cys32. Conformation-sensitive Raman bands of tryptophan, of Asp and Glu carboxylate groups, and of aliphatic side chains indicate significant changes in environments and interactions of these side chains with thiol titrations, even though the native secondary structure of thioredoxin is largely conserved to pH 7.9. At pH 12.2, corresponding to the dithiolate form of the protein, large changes are observed in several Raman bands, indicating that more substantial changes in secondary and tertiary structure accompany dithiolation of the active center. Both the reduced and oxidized forms of thioredoxin exhibit Raman amide I at 1668 cm^{-1} and amide III at 1248 cm^{-1}, consistent with a peptide backbone rich in the β-sheet conformation and largely invariant to the oxidation state of the active-center cysteines. If differences exist between secondary structures of the two forms, they are below the level (<2%) that can be differentiated on the basis of the Raman amide bands. However, significant differences are observed in Raman bands of many amino acid side chains, indicating substantial changes in side-chain environments with oxidation. The disulfide Raman marker (S–S stretching band) of aqueous thioredoxin is observed at 507 cm^{-1}, diagnostic of an all-gauche C–C–S–S–C–C rotamer and consistent with the crystal structure.

Escherichia coli thioredoxin is one of a large family of small proteins containing a redox-active pair of cysteines capable of catalyzing enzyme-specific disulfide reduction (Laurent et al., 1964). Thioredoxin is also implicated in pathways of bacteriophage morphogenesis, including assembly of filamentous phages M13 and f1, where it may perform structural rather than catalytic functions (Russel, 1991). The active center of *E. coli* thioredoxin, -Cys32-Gly33-Pro34-Cys35-, is located within the acidic N-terminal third of the 108-residue polypeptide chain. The oxidized disulfide form of the protein [$TRX(S)_2$][1] is reduced to the dithiol form [$TRX(SH)_2$] with evidence of conformational changes localized in the vicinity of the active center (Dyson et al., 1990; Reutimann et al., 1981; Merola et al., 1989). Biochemical and structural studies of thioredoxin have been reviewed by Holmgren (1985, 1989).

The high-resolution crystal structure of $TRX(S)_2$ has been solved at pH 3.8 (Katti et al., 1990). The protein fold consists essentially of a five-stranded β-sheet core, flanked by four α-helical segments. Thioredoxin contains only two cysteine residues, Cys32 and Cys35, and these form the active-site disulfide bridge which is located in a reverse turn between the central β-strand and the α_2-helix. The side-chain atoms of Cys32 and Cys35 are mostly buried. In the vicinity of the disulfide is the buried carboxylic acid side chain of Asp26, which is completely conserved among thioredoxins. Only one oxygen atom of the Asp26 side chain is partially exposed to solvent, through a deep cleft reaching in from the surface. The pK_a of the Asp26 side chain in $TRX(S)_2$ was shown to be 7.5 (Langsetmo et al., 1991a). The perturbation of the Asp26 pK_a is due primarily to the desolvation penalty associated with charging the carboxyl group in a hydrophobic environment (Langsetmo et al., 1991b). The structural effect of charging Asp26 at physiological pH is not known, since the crystal structure was determined at pH 3.8 where Asp26 is fully protonated.

The crystal structure of $TRX(SH)_2$ has not been solved. However, the NMR structure has been reported (Dyson et al., 1990) and indicates no significant differences from the $TRX(S)_2$ structure except in the region of the active site. Recent tritium exchange studies (Kaminsky & Richards,

† Supported by NIH Grant AI11855.

* Author to whom correspondence may be addressed.

‡ University of Missouri—Kansas City.

§ University of Minnesota.

[1] Abbreviations: $TRX(SH)_2$, reduced (dithiol form) of thioredoxin; $TRX(S)_2$, oxidized (disulfide form) of thioredoxin; IPTG, isopropyl β-D-thiogalactopyranoside; EDTA, ethylenediaminetetraacetic acid; DTT, dithiothreitol; FWHM, full-width at half-maximum.

0006-2960/93/0432-5800$04.00/0

1992a) and sound velocity experiments (Kaminsky & Richards, 1992b) suggest that there are significant differences between $TRX(S)_2$ and $TRX(SH)_2$, particularly at the protein–solvent interface, and that these are not necessarily limited to the active-site region. Gleason (1992) suggests that the role of Asp26 may be to provide an electrostatically compatible surface for other proteins with which thioredoxin interacts, rather than to function directly as an intramolecular site in proton translocation.

A key element in mechanisms proposed for thioredoxin oxidoreductase activity [reviewed in Holmgren (1989)] is the formation in $TRX(SH)_2$ of a thiolate anion (S^-) at physiological pH. Presumably, the thiolate species serves as the nucleophile for initial attack on the disulfide bridge of the protein being reduced by thioredoxin. The presence of a thiolate ion at physiological pH implies that at least one cysteine has a pK_a below 8.3, the typical value for a free cysteine SH. A range of values has been reported for the two pK_a's of the thioredoxin cysteine thiols. Reutimann et al. (1981) observed a titration of tryptophan fluorescence intensity in $TRX(SH)_2$ with a pK_a of 6.4 and ascribed this to one of the two active-site thiols. From experiments on the alkylation of the sulfhydryls, which requires the thiolate species, and the pH dependence of alkylation, Kallis and Holmgren (1980) assigned a pK_a of 6.7 to Cys32 and a pK_a of about 9 to Cys35. From the pH dependence of the NMR chemical shifts of a number of protons in the vicinity of the active site, Dyson et al. (1991) assigned a pK_a of 7.1–7.4 to both the Cys32 thiol and Asp26 carboxyl, and a pK_a of 8.4 to the Cys35 thiol. In human thioredoxin, which shares the general structure of *E. coli* thioredoxin, but also has significant differences in ionizable groups in the vicinity of the active site, pK_a values of 6.3 (Cys32) and 7.5–8.6 (Cys35) have also been determined by NMR (Forman-Kay et al., 1992).

We have employed laser Raman spectroscopy to monitor directly the thioredoxin sulfhydryl groups. We observe two components to a complex Raman SH band envelope in $TRX(SH)_2$. The two band components are assigned to the two cysteine thiols. From the decrease in intensity of these bands with increasing pH, we have determined the pK_a values of both cysteines in $TRX(SH)_2$. It is clear that each titrates with $pK_a < 8.2$. Quantitative decomposition of the SH band components at varying pH indicates that the pK_a values of the cysteine thiols are approximately 7.1 and 7.9.

We have also examined other regions of the Raman spectrum to assess changes in solution secondary (α-helix and β-sheet) and tertiary structures (side-chain environments and configurations) accompanying titration of the ionizable cysteines. Finally, we have employed Raman spectroscopy to compare the solution structures of both oxidized and reduced forms of thioredoxin.

EXPERIMENTAL METHODS

Proteins. Wild-type *E. coli* thioredoxin was purified from *E. coli* strain JF521 containing the plasmid pTK100 which overexpresses the trxA gene. Construction of this plasmid and *E. coli* strain have been described (Langsetmo et al., 1989). Thioredoxin was purified from a 6-L culture of cells. After overnight growth, thioredoxin synthesis was induced with 3 mM isopropyl β-D-thiogalactopyranoside (IPTG). After an additional 2 h of incubation, cells were chilled, centrifuged, resuspended in 30 mM Tris/1 mM ethylenediaminetetraacetic acid (EDTA), pH 8.4, and sonicated. Following sonication, cell debris was removed by centrifugation, and one-fifth final volume of a 10% streptomycin sulfate suspension was added to the supernatant which was stirred overnight at 4 °C. The streptomycin sulfate precipitate was removed by centrifugation, and the supernatant was passed through a 0.22-μm Millipore filter. The sample was chromatographed first on a Pharmacia S-100 size-exclusion column and subsequently on an EM Separations Fractogel EMD DEAE-650 (M) ion-exchange column eluted with a 0–0.15 M NaCl gradient. Pooled thioredoxin fractions were concentrated and exchanged into 30 mM Tris/1 mM EDTA, pH 8.4, using an Amicon 8400 concentrator equipped with a YM3 filter, and stored at −70 °C.

Thioredoxin solutions were prepared for Raman spectroscopy by addition of reduced dithiothreitol (DTT) to 100 mM. The solution was stirred at 20 °C for 1 h under N_2 and then applied to a Pharmacia Sephacryl S-100 size-exclusion column, preequilibrated with deaerated column buffer. For samples in the range pH 7–13, column buffers were 10 mM Tris at the specified pH, with 1 mM EDTA and 3 mM β-mercaptoethanol. For pH 4 experiments, 10 mM succinate was substituted for Tris. Before use, buffers were deaerated and subsequently saturated with N_2. During elution, column buffers in the reservoir were bubbled with N_2. The thioredoxin peak was concentrated under N_2 using an Amicon 8MC concentrator equipped with a YM3 filter. The pH of concentrated thioredoxin samples was determined using a Corning 240 pH meter with a semimicro combination electrode. Thioredoxin concentrations were determined spectrophotometrically using an extinction coefficient at 280 nm of 13 700 mol^{-1} cm^{-1} (Lundstrom et al., 1992). Samples (20–100 μL) were sealed in 1-mm glass capillary tubes (Kimax no. 34502) under N_2 and stored in the cold until spectra were recorded.

Raman Spectroscopy. Raman spectra were excited in the 90° scattering geometry with 200 mW of 514.5-nm laser excitation (Coherent Innova-70) and recorded on a scanning spectrophotometer (Spex Ramalog 1401). Data were collected at 1.0-cm^{-1} intervals with 2.0-s integration time and 8-cm^{-1} spectral slit width. Liquid indene was employed to calibrate Raman frequencies to within 1 cm^{-1} in the intervals 300–1800 and 2700–3700 cm^{-1}. For the region 2300–2700 cm^{-1}, *in situ* N_2 was employed to calibrate sulfhydryl Raman frequencies to within ±0.5 cm^{-1}. We observed the distinctive and sharp N_2 Raman band at 2330.7 cm^{-1} (Herzberg, 1950), which results from air near the focus of the laser beam and which fortuitously exhibits a Raman scattering cross section comparable to that of thioredoxin sulfhydryls (Li et al., 1993). The N_2 Raman band was also exploited as an intensity standard (see below). All Raman frequencies are reported to an accuracy of 1 cm^{-1}.

Raman spectra of thioredoxin were obtained from solutions (≈80–150 $\mu g/\mu L$) sealed at ambient pressure in 1-mm glass capillary cells, as described above. Cells were thermostated at 6 °C in the sample illuminator of the spectrometer (Thomas & Barylski, 1970) while data were collected. Solvent and scattering backgrounds were subtracted from the signal-averaged spectra by difference methods described elsewhere (Verduin et al., 1984). Fourier deconvolution and curve-fitting procedures were carried out using software developed in our laboratory and described previously (Thomas & Agard, 1984).

In the computation of thioredoxin difference spectra, intensities of minuend and subtrahend were normalized to minimize differences in bands considered to be essentially invariant in intensity, e.g., the bands at 1450 and 1002 cm^{-1}, assigned respectively to aliphatic CH_2 scissoring modes and

phenyl ring stretching of phenylalanine residues. As often observed for other proteins (Thomas et al., 1986), this procedure leads also to conservation of the integrated intensities of amide I and amide III bands and minimization in the total number of difference bands. Difference peaks and troughs were not considered significant unless they exhibited at least 2-fold greater intensity than the base-line noise level. Further details of instrumentation, software, and related experimental methods have been described (Li et al., 1992a).

Spectrophotometric Determination of Sulfhydryl Concentration. Accurate and precise determination of cysteine sulfhydryl concentration from the Raman spectrum is described in detail elsewhere (Li et al., 1993). In brief, the integrated intensity of the Raman SH stretching band (2550–2570-cm^{-1} interval) is normalized to that of the Raman N_2 band to establish SH band intensity in a given solution of thioredoxin. The normalized SH band intensity so obtained from a thioredoxin solution at given pH can be expressed as moles of thiol per mole of protein by normalization to the total protein concentration in solution, as determined from the relative intensity of the Raman band envelope (2800–3000-cm^{-1} region) due to CH stretching of all protein aliphatic groups. The total protein concentration is proportional to the relative intensities of protein CH stretching bands (2800–3000 cm^{-1}) and solvent OH stretching bands (3000–3700 cm^{-1}). Corrections for traces of oxidized protein, if required, can be made by an appropriate analysis of the Raman S–S stretching band intensity at 507 cm^{-1} (Lord & Yu, 1970).

In the present work, significant oxidation was prevented by addition of a small amount of β-mercaptoethanol (3 mM) to $TRX(SH)_2$ solutions. Independent experiments demonstrated that the Raman S–H band of β-mercaptoethanol (2580 cm^{-1}) is well removed from the center of the thioredoxin S–H band complex and produces no measurable Raman intensity vis-a-vis the N_2 band as long as the β-mercaptoethanol concentration is not greater than 5 mM. [In the $TRX(SH)_2$ solutions studied here, the effective sulfhydryl concentration is within the range 15–25 mM.] We also demonstrated a strictly linear relationship between the Raman S–H band intensity and mercaptan concentration over several orders of magnitude (0.006–1.5 M). Additionally, we verified that the Raman intensity of the external N_2 standard is accurately reproducible at constant atmospheric pressure and invariant to sample concentration, temperature, and pH in the sealed cells employed for these experiments (Li et al., 1993).

RESULTS AND DISCUSSION

The structural conclusions reached in the present work are based upon previous empirical (Li & Thomas, 1991) and theoretical (Li et al., 1992b) studies of cysteine and related model compounds, which correlate the Raman SH band with specific hydrogen-bonding states of the S–H donor group and configurations of the CαH–C$\beta$$H_2$–S–H side chain of cysteine. Quantitative interpretation of the results on thioredoxin sulfhydryls is accomplished by accurate measurement of frequencies and intensities of the intrinsically strong Raman SH bands, as outlined in the following sections. A more detailed description of the Raman spectrophotometric methodology, which exploits the Raman-active stretching mode (2330.7-cm^{-1} band) of N_2 as an intensity and frequency standard, is given elsewhere (Li et al., 1993).

Raman Spectra and Assignments for Thioredoxin

The complete Raman spectrum (500–3700 cm^{-1}) of $TRX(SH)_2$ in H_2O solution at pH 4.0 is shown in Figure 1. Specific regions of the spectrum, which are discussed separately below, are described in the Figure 1 legend.

Table I: Raman Frequencies, Intensities, and Assignments of Reduced and Oxidized *E. coli* Thioredoxin[a]

$TRX(SH)_2$		$TRX(S)_2$		
frequency	intensity	frequency	intensity	assignment[b]
418	1.2	421	1.0	
		507	1.0	SS str ($g^-/g^-/g^-$)
535	1.0	539	1.0 b	
563	1.5	565	1.5	amide VII
592	0.5 s	591	0.5 s	
618	1.1	620	1.0	F
642	0.8	643	0.8	Y
675	0.5	668	0.7	CS stretch
701	0.5	704	0.4	CS stretch
755	4.9	756	4.8	W
777	1.2 s	778	0.9 s	
800	0.4	801	0.4	
827	2.5	827	2.4	Y
853	1.3	853	1.3	Y
881	1.0	881	1.1	W
898	0.9	898	0.9	CCC bend
934	2.3	933	2.6	CCC bend
956	1.3	954	1.4	CCC bend
1003	8.8	1003	9.2	F
1012	3.4 s	1012	3.7 s	W
1032	1.4	1032	1.5	F
1064	1.7	1062	1.5	CC, CN, CO stretch
1081	1.8 b	1081	1.5 b	CC, CN stretch
1103	1.1	1104	1.2	CC stretch
1128	2.8	1128	2.9	CC stretch
1157	1.0	1156	1.0	CC stretch
1173	1.2	1173	1.3	
1209	4.7	1208	4.8	Y
1231	4.2 s	1232	4.2 s	amide III
1246	6.4	1246	6.2	amide III
1288	4.9 bs	1288	4.8 bs	amide III
1307	5.0	1308	4.9	CH bend
1321	6.6 b	1321	6.4	CH bend
1339	8.6	1339	8.5	W, CH bend
1361	2.8 s	1360	3.0 s	W
1400	3.1	1399	2.5	COO^- stretch
1422	2.7	1423	2.6	CH bend
1450	10.0	1450	10.0	CH bend
1465	7.8 s	1466	7.5 s	CH bend
1547	3.3	1546	3.1	W
1578	1.6 s	1578	1.2 s	W
1586	1.6	1591	1.4	
1607	4.0	1607	3.9	F, Y
1618	3.5	1618	3.7	Y, W
1665	10.9	1665	11.5	amide I
2569				SH stretch
2876		2876		aliphatic CH stretch
2937		2937		aliphatic CH stretch
2970		2970		aliphatic CH stretch
3067		3067		aromatic CH stretch

[a] Frequencies are in cm^{-1} units; intensities are arbitrary on a 0–10 scale. Abbreviations: s = shoulder, b = broad band. [b] Only major contributors are indicated. See also the text.

Raman spectra in the region 300–1750 cm^{-1} of $TRX(SH)_2$ and $TRX(S)_2$ at pH 7.0 are compared in Figure 2. Labels indicate Raman frequencies of several prominent peaks, which are further discussed in the following sections. A complete tabulation of Raman band frequencies and assignments is given in Table I. The most intense Raman band of thioredoxin is due to the amide I mode, centered at 1665 cm^{-1}. Other intense Raman bands originate from amide III (centered near 1246 cm^{-1}), ring vibrations of aromatic side chains (Phe at 618, 1003, 1032, and 1607 cm^{-1}; Tyr at 642, 827, 853, and 1618 cm^{-1}; Trp at 755, 881, 1012, 1339, 1361, 1547, and 1578 cm^{-1}), methyl and methylene deformations (1321, 1339, 1422, and 1450 cm^{-1}), S–H stretching (2569 cm^{-1}), and aliphatic C–H stretching (2876, 2937, and 2970 cm^{-1}).

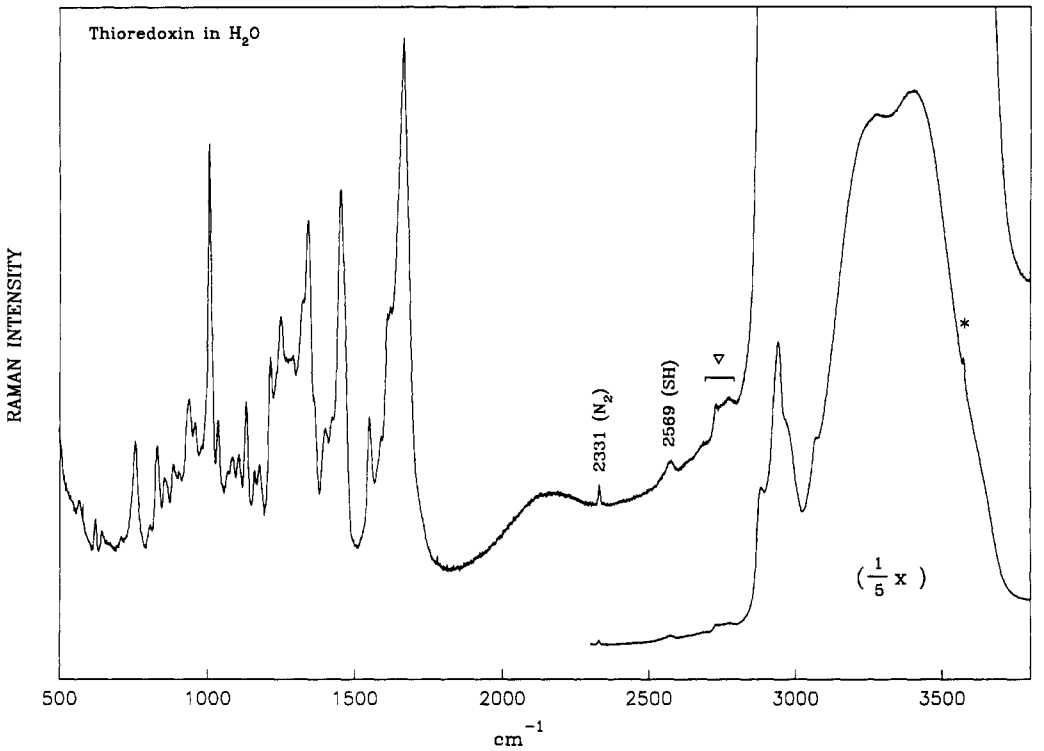

FIGURE 1: Raman spectrum in the region 500–3700 cm^{-1} of reduced thioredoxin at pH 4 and 6 °C (sequence: ^{1}SDKIIHLTDD^{11}SFDTD-VLKAD^{21}GAILVDFWAE^{31}WCG PCKMIAP^{41}ILDEIADEYQ^{51}GKLTVAKLNI^{61}DQNPGTAPLY^{71}GIRGIPTLL-L^{81}FKNGEVAATK^{91}VGALSKGQLK^{101}EFLDANLA). Protein concentration is ≈100 μg/μL. The Raman band of N_2 at 2331 cm^{-1} serves as a frequency and intensity reference. The complex Raman band at 2569 cm^{-1} is due to Cys32 and Cys35 sulfhydryl stretching modes. Raman bands just below 3000 cm^{-1}, which are due to aliphatic CH stretching modes of most side chains and the very broad, complex band of H_2O solvent *ca.* 3400 cm^{-1}, are evident in the segment recorded at one-fifth amplification. The symbols (∇) and (*) indicate probable overtone/combination bands and a laser emission line, respectively. The region 500–1800 cm^{-1}, which contains amide I and III conformation markers and most side-chain Raman bands, is shown on expanded scales in Figures 2 and 3, below.

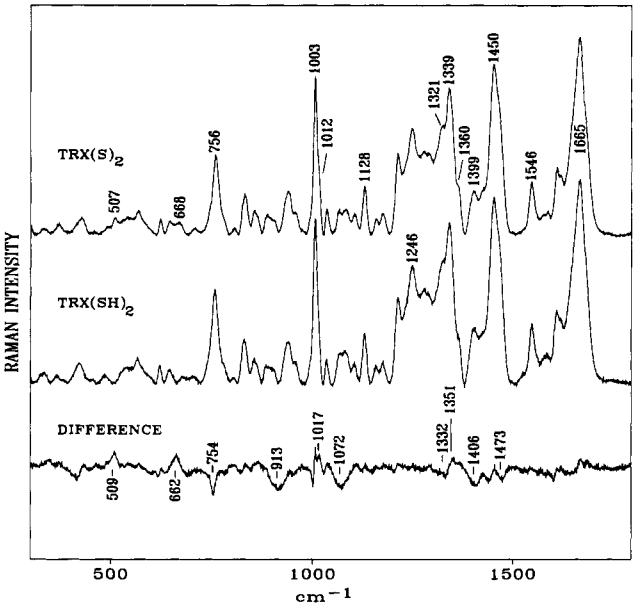

FIGURE 2: Raman spectra in the region 300–1750 cm^{-1} of oxidized (top) and reduced (middle) thioredoxin at pH 7.0 and 6 °C, and their difference spectrum (bottom). Protein concentrations are ≈120 μg/μL. Labels indicate frequencies of difference bands (peaks and troughs) which are discussed in the text.

Solution Structures of TRX(SH)$_2$ and TRX(S)$_2$

Secondary Structure. TRX(S)$_2$ and TRX(SH)$_2$ exhibit nearly identical amide I and amide III profiles, as shown in Figure 2. This is consistent with other reports that the solution secondary structure of thioredoxin does not change substantially with oxidation state. The observed peak positions for amide I (1665 cm^{-1}) and amide III (1246 cm^{-1}) indicate that the secondary structure is dominated by β-sheet (Yu et al., 1973; Chen & Lord, 1974). A contribution to amide I from turns or β-strand may generate the apparent amide I shoulder *ca.* 1675–1680 cm^{-1} (Thomas et al., 1987). A component to amide I from the significant α-helix structure of thioredoxin, expected on the low-frequency side of the amide I peak, is not resolved experimentally but is revealed by Fourier deconvolution as a satellite *ca.* 1655 cm^{-1} (not shown) (Thomas & Agard, 1984). The Figure 2 difference spectrum shows a very weak trough (*ca.* 1655 cm^{-1}) and peak (*ca.* 1675 cm^{-1}) in the amide I region, suggesting that oxidized thioredoxin may contain marginally less (<2%) α-helix or irregular structure and correspondingly more β-strand or turn than reduced thioredoxin. The deconvolved Raman amide bands of aqueous TRX(S)$_2$ and TRX(SH)$_2$ are consistent with ≈75% of residues in well-defined secondary structure, in accordance with the NMR solution structure (Dyson et al., 1990) and X-ray crystal structure (Katti et al., 1990).

The difference spectra of Figure 3 show that the solution secondary structure of TRX(SH)$_2$ does not change in the pH range 4.0 < pH < 7.9 but changes significantly in the range 7.9 < pH < 12.2.

Side Chains. Figure 2 indicates a number of spectral differences between TRX(S)$_2$ and TRX(SH)$_2$, which are due exclusively to side chains. The band at 507 cm^{-1} in TRX(S)$_2$, absent from TRX(SH)$_2$ and responsible for the difference peak at 509 cm^{-1}, identifies the disulfide bridge of TRX(S)$_2$ and indicates the all-gauche C–C–S–S–C–C network (Sugeta et al., 1972, 1973; Van Wart & Scheraga, 1986). The prominent shoulder at 668 cm^{-1} in TRX(S)$_2$, assigned to C–S

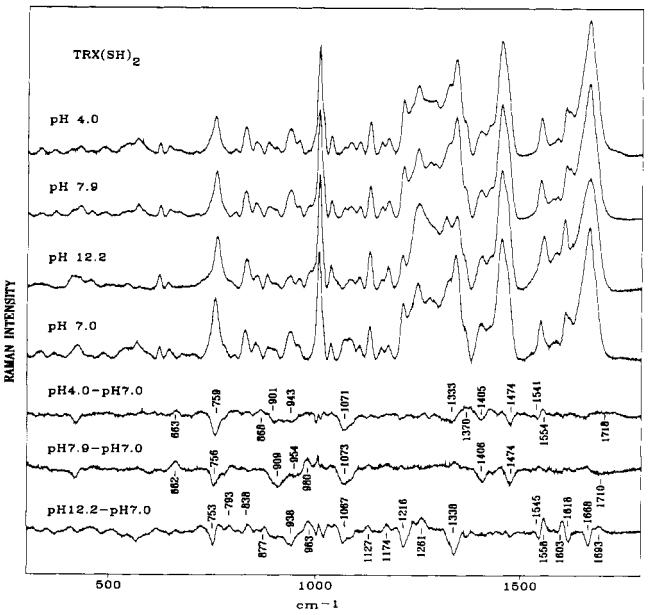

FIGURE 3: From top to bottom: Raman spectra in the region 300–1800 cm^{-1} of reduced thioredoxin at pH 4.0, 7.9, 12.2, and 7.0, and difference spectra between pH 7.0 (subtrahend) and other pH values (minuends). Labels indicate frequencies of the principal difference bands.

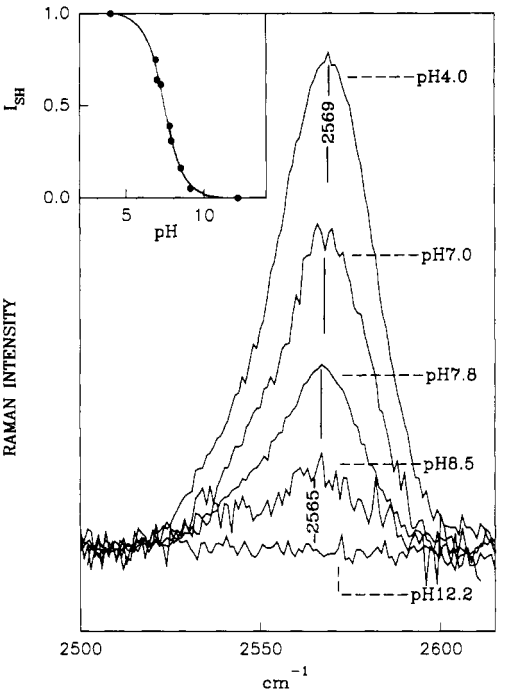

FIGURE 4: Raman spectra in the 2500–2625-cm^{-1} region of reduced thioredoxin at the indicated pH values. The bottom trace, obtained at pH 12.2 for which all sulfhydryls are titrated to thiolate ion, indicates the level of background noise in this region of the spectrum. The spectra obtained at pH 4.0 and 7.8 represent averages of 300 scans. Other spectra represent averages of 55 scans. The inset (upper left) shows a Raman–pH titration curve obtained from these spectra and additional data not shown. The ordinate in the titration curve is the normalized, integrated intensity of the total Raman SH band.

stretching of the disulfide, is also diagnostic of the gauche rotamers (Sugeta et al., 1972).

The trough at 754 cm^{-1} in the Figure 2 difference spectrum, which results from the higher intensity of the 755-cm^{-1} tryptophan band in $TRX(SH)_2$, suggests a more hydrophilic environment for the average indole ring of reduced thioredoxin (Miura et al., 1991). The observed change of relative intensity in the two members of the tryptophan Fermi doublet (sharp peak near 1339 cm^{-1} and shoulder near 1360 cm^{-1}) confirms that the tryptophans of $TRX(SH)_2$ exist in a more hydrophilic ring environment (Harada et al., 1986). The tyrosine Fermi doublet at 853 and 827 cm^{-1} (Siamwiza et al., 1975) exhibits the same intensity ratio ($I_{853}/I_{827} \approx 0.50$) in both $TRX(SH)_2$ and $TRX(S)_2$, diagnostic of strong phenolic OH donors for both forms of the protein. The Raman band near 1400 cm^{-1} is assignable to the symmetric stretching vibration of ionized carboxylate groups (CO_2^-). The higher intensity observed for the 1400-cm^{-1} band of $TRX(SH)_2$ implies either a larger percentage of ionized carboxyls in the reduced state of thioredoxin or differences in average local environments for carboxylates of $TRX(SH)_2$ and $TRX(S)_2$. Although specific structural correlations do not exist for the difference bands near 913, 1072, and 1473 cm^{-1}, these suggest significant environmental and/or conformational changes in a variety of side chains with oxidation. Raman bands of many specific side chains of $TRX(SH)_2$, including those of Cys, Trp, Tyr, Asp, and Glu residues, are discussed in more detail in the next section.

pH Titration of Reduced Thioredoxin

The difference spectra of Figure 3 reveal that although the secondary structure of $TRX(SH)_2$ is not strongly dependent upon pH in the range 4.0 < pH < 7.9, interactions and environments of many side chains are greatly affected by pH titration. This suggests either changes in internal packing, perhaps between secondary structure domains, or changes in the solvent–protein interface, or both, over the range of pH investigated. In this section, we identify the Raman bands which exhibit pH sensitivity and interpret the structural significance of the observed intensity and frequency changes.

Thiol → Thiolate Equilibria of Cys32 and Cys35. Figure 4 shows the complex and asymmetric Raman sulfhydryl band observed for reduced thioredoxin in solutions of different pH. At pH 4.0, where both Cys32 and Cys35 are fully protonated, the band exhibits maximum integrated intensity, and its peak is observed at 2569 cm^{-1}. (We have verified that oxidized thioredoxin is not present in significant amounts in these solutions by monitoring the spectral region 500–550 cm^{-1} which reports the S–S stretch.) As the pH is increased, the intensity of the sulfhydryl band decreases, reaching zero at the high-pH limit of 12.2. Included in Figure 4 (inset, upper left) is a plot of the normalized, integrated sulfhydryl Raman band intensity vs solution pH. The data indicate that the intensity is diminished by 50% at pH 7.5, which represents the apparent average pK_a for the two thiol → thiolate equilibria. The Figure 4 spectra show further that the experimentally measured SH band center (peak bisector) shifts by a small but significant amount to lower frequency as the pH is increased. This is consistent with the contribution of two populations of inequivalent sulfhydryls to the composite Raman band, and with the higher frequency component titrating preferentially to the thiolate form as the pH is increased. In order to distinguish the two pK_a values corresponding to Cys32 and Cys35 thiolate formation, we have decomposed the complex and asymmetric Raman SH band into two components as follows.

In Figure 5 (left panel), the experimental pH 4.0 sulfhydryl spectrum is fitted to two Gauss–Lorentz components, subject to the imposed constraint of equal integrated intensity for each component. This is in accordance with model compound studies showing that sulfhydryls which are distinguished by

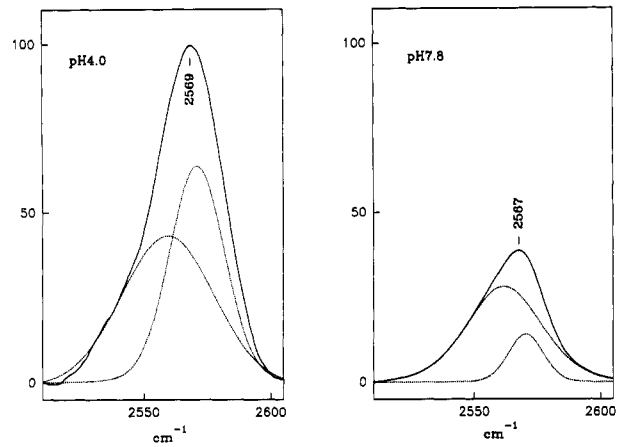

FIGURE 5: Least-squares fit of the complex Raman sulfhydryl band of reduced thioredoxin at pH 4.0 (left panel) and pH 7.8 (right panel) to Gauss–Lorentz functions. The component bands are centered at 2562 ± 1 and 2571 ± 1 cm^{-1}, and the lower frequency component exhibits the larger bandwidth, consistent with a more strongly hydrogen-bonded S–H donor. See text.

different environments (i.e., intrinsically different S–H stretching frequencies) exhibit equal Raman band intensities per unit of molecular concentration (Li & Thomas, 1991). The component of lower frequency occurs at 2562 cm^{-1} and is relatively broad, exhibiting a full-width at half-maximum (FWHM) of 36 cm^{-1}. The component of higher frequency occurs at 2571 cm^{-1} with a FWHM of 26 cm^{-1}. These results are consistent with the presence of two fully protonated sulfhydryls in $TRX(SH)_2$, both of which are moderate to strong hydrogen-bond donors, but one of which (marker at 2562 cm^{-1}; FWHM = 36 cm^{-1}) is more strongly hydrogen-bonded than the other (marker at 2571 cm^{-1}; FWHM = 26 cm^{-1}) (Li & Thomas, 1991).

The Raman spectra do not indicate whether Cys32 or Cys35 is the stronger hydrogen-bond donor. However, Raman SH frequencies of 2562 and 2571 cm^{-1} are observed for SH groups hydrogen-bonded, respectively, to carboxyl and water (or hydroxyl) oxygens (Li & Thomas, 1991; H. Li and G. J. Thomas, Jr., unpublished results). In the NMR structure of reduced thioredoxin (Dyson et al., 1990), Cys35 is close enough to Asp26 to donate a hydrogen bond to the carboxylate C=O acceptor. Therefore, we tentatively assign the more strongly hydrogen-bonded sulfhydryl (marker at 2562 cm^{-1}) to Cys35 and the lesser donor to Cys32.

Also shown in Figure 5 (right panel) are the results of curve-fitting the experimentally observed pH 7.8 sulfhydryl band to the same two components employed above for fitting the pH 4.0 spectrum. At pH 7.8, the experimental band can be reproduced satisfactorily only if the more strongly hydrogen-bonded sulfhydryl (2562 cm^{-1}) contributes a much more intense Raman band than the less strongly hydrogen-bonded sulfhydryl (2571 cm^{-1}). The optimum fit of the band envelope requires the intensity ratio I_{2562}/I_{2571} = (4.4 ± 0.4):1.0, as shown in Figure 5. This indicates that the two pK_a values are separated by 0.6–0.9 unit, or $pK_1 = pK_{C32} = 7.1 \pm 0.2$ and $pK_2 = pK_{C35} = 7.9 \pm 0.2$ for the respective thiol → thiolate equilibria. The deviations represent both the range of pK_a calculated from duplicate runs at pH 7.8 and uncertainties in the spectral intensity measurements. The sulfhydryl bands observed for other thioredoxin solutions in the range 4 < pH < 8 (Figure 4 and additional data not shown) are consistent with the pK_1 and pK_2 values calculated from the pH 7.8 data. The pH titration results are summarized in Table II.

Table II: Summary of Conformational and Structural Properties of Reduced and Oxidized Thioredoxin

oxidation state	pH	Cys32 SH:S⁻ ratio	Cys35 SH:S⁻ ratio	X^1(Cys)	$\|X^{2,1}\|$(Trp) (deg)	carboxyl state(s)
$TRX(S)_2$	6.96			G′	85	COOH < COO^-
$TRX(SH)_2$	4.00	100:0	100:0	G′	85	COOH
	6.96	56:44	14:85	T	85[a]	COOH < COO^-
	7.90	90:10	50:50	G′	85[a]	COO^-
	12.20	0:100	0:100	G′	110	COO^-

[a] The date indicate a small population (≈25%) of tryptophan residues at this pH with $|X^{2,1}| \approx 110°$. See Figure 3 and discussion in text.

Cysteine Side-Chain Conformation. Studies of model compounds show that the C–S stretching frequency (σ_{CS}) of the cysteinyl side chain is highly sensitive to changes in the Cα–Cβ torsion (X^1) of the N–Cα–Cβ–S network. For a rotamer in which the Cα hydrogen is trans to sulfur (T′), σ_{CS} is expected near 660 cm^{-1}; for a gauche rotamer (G′), σ_{CS} can be 50–100 cm^{-1} higher (Nogami et al., 1975a,b; Ozaki et al., 1975; Li et al., 1992b). The σ_{CS} marker, though not sensitive directly to thiolate ion formation, should reflect conformational changes in X^1 resulting from thiolation. The $TRX(SH)_2$ difference spectra of Figure 3 show features near 660–665 cm^{-1} which imply pH-related changes in σ_{CS} due to changes in X^1, presumably a consequence of thiolate ion formation. (Spectral changes near 750–760 cm^{-1} are also observed in the Figure 3 difference spectra, but these probably represent the combined effects of changes in cysteine Cα–Cβ torsion and indole ring environments, with the latter dominating.) Between pH 4.0 and pH 7.0, as the less strongly hydrogen-bonded cysteine (Cys32) is preferentially titrated, the Raman intensity near 663 cm^{-1} is diminished. This indicates a decrease, between pH 4 and 7, in the total population of trans rotamers. The conformational change may occur in either Cys32 or Cys35, or in both. A simultaneous intensity increase occurs near 759 cm^{-1}, consistent with an increase in gauche rotamers, but it is not clear whether the 759-cm^{-1} difference band is due to cysteine C–S stretching because of the intense tryptophan band overlapping the σ_{CS} marker.

Tryptophan Conformations and Interactions. Figures 2 and 3 show that the tryptophan residues, Trp28 and Trp31, are prominent contributors to the Raman spectrum of thioredoxin. Structural correlations exist for the Raman bands near 755–760, 875–881, 1340/1360, and 1545–1555 cm^{-1} (Kitagawa et al., 1979; Harada et al., 1986; Miura et al., 1989, 1991). Since these result from both Trp28 and Trp31, they provide information generally about the average environment of both residues. Nevertheless, specific structural conclusions may be reached as follows.

At pH 4.0, the 1547-cm^{-1} band (Table I) indicates that the magnitude of the C3–Cβ torsion angle ($|X^{2,1}|$) is approximately 85° for both tryptophan side chains in the dithiol form of thioredoxin (Miura et al., 1989). The bandwidth is narrowest at pH 4 (Figure 3), showing that the $|X^{2,1}|$ values for Trp28 and Trp31 are most nearly equal at pH 4. At pH 6.96, a fraction (≈25%) of the band intensity is shifted to higher frequency (1554 cm^{-1}), denoting an increase of $|X^{2,1}|$ to ≈110° for this fraction of tryptophan residues. Tryptophan fluorescence measurements (Reutimann et al., 1981) suggest that this conformational change may occur mainly in Trp28. Although no additional change is apparent between pH 6.96 and pH 7.90 (Figure 3), the entire tryptophan band is shifted to 1554 cm^{-1} at pH 12.2, which implies that both Trp28 and

Trp31 exhibit $|\chi^{2,1}| \approx 110°$ in the dithiolate form of thioredoxin. These findings are summarized in Table II.

Tryptophan generates a Fermi doublet at 1360 and 1340 cm^{-1}, with a relative intensity ratio (I_{1360}/I_{1340}) sensitive to the hydropathic environment of the indole ring (Rava & Spiro, 1985; Harada et al., 1986). For a hydrophilic indole, I_{1360}/I_{1340} is typically low; for a hydrophobic indole, I_{1360}/I_{1340} is high. All spectra of Figure 3 exhibit a low value of I_{1360}/I_{1340}, diagnostic of relatively hydrophilic environments for the average indole ring. Additionally, indole hydrophilicity is somewhat greater near pH 7 than at pH 4. We note that in the pH 12.2 spectrum, the dramatic intensity decrease *ca.* 1338 cm^{-1} occurs without a concomitant increase at 1360 cm^{-1}, and therefore cannot be attributed simply to the tryptophan Fermi doublet. The pH 12.2 data probably reflect a change in secondary structure, as well as changes in environments of many different side chains. The tryptophan band near 755 cm^{-1} is also regarded as sensitive to the indole ring environment, though the relationship is apparently more complex and not well understood (Miura et al., 1991). Figure 3 shows that the 755-cm^{-1} band of $TRX(SH)_2$ is highly sensitive to pH, shifting to lower frequency (753 cm^{-1}) and exhibiting markedly lower intensity at pH 12.2.

A characteristic tryptophan band near 875–881 cm^{-1} is, in principle, sensitive to the strength of indole 1N–H hydrogen-bond donation (Miura et al., 1991). In thioredoxin, the band occurs consistently at high frequency (*ca.* 881 cm^{-1}), indicative of very weak 1NH hydrogen-bonding. However, this tryptophan marker is overlapped considerably by a band near 900 cm^{-1}, the latter due probably to aliphatic side chains. Because of this extensive band overlap, detailed interpretation of the pH dependence of the 881-cm^{-1} band is not feasible. Nevertheless, the spectra of Figure 3 show that the relative intensity and half-width of the 881-cm^{-1} band are pH-dependent, suggesting that indole NH interactions differ in the dithiol, thiol, and thiolate forms of thioredoxin. We note, particularly, that the band is best resolved in the pH 12.2 spectrum, where it exhibits a peak position at *ca.* 877–879 cm^{-1}, marginally lower than in thiol forms, implying somewhat stronger NH hydrogen-bonding for the dithiolate form. This effect presumably explains the appearance of the positive difference band at *ca.* 877 cm^{-1} in the pH 12.2 – pH 7.0 difference spectrum of Figure 3.

Collectively, the above results show that conformational changes occurring in the active center of thioredoxin as a function of solution pH also affect the average molecular environment and interactions of Trp28 and Trp31. Specifically, the representative indole ring environment is more hydrophilic and the 1N–H group is a stronger hydrogen-bond donor at pH 7–8 than at pH 4. Additionally, the tryptophan side-chain torsion ($|\chi^{2,1}|$), which has a value of 85° for all residues at pH 4, is increased to ≈110° for a minority of tryptophan residues near pH 7, and for all tryptophans at pH 12.2.

Tyrosine Interactions. The two tyrosines of thioredoxin, Tyr49 and Tyr70, are well removed from the active center and located within reverse turns which occur near the surface of the protein tertiary fold. The tyrosine Fermi doublet intensity ratio I_{853}/I_{827} is 0.50 ± 0.05, irrespective of pH (Figure 3). This denotes strong hydrogen-bond donation by the phenolic OH group of each tyrosine and confirms that the phenolic hydrogen-bonding states are essentially unaffected by thiolate formation. Since a tyrosine phenoxyl group exposed to H_2O is characterized by an intensity ratio $I_{853}/I_{827} = 1.25$ (Siamwiza et al., 1975), neither Tyr49 nor Tyr70 is fully exposed to solvent, and neither accepts a hydrogen bond from an OH or NH donor. The Raman results, therefore, indicate that both tyrosines are sufficiently buried to prevent solvent contact, and each donates a strong hydrogen bond to an appropriate acceptor, such as C=O of a peptide group or side chain.

Aspartate and Glutamate Side Chains. Aspartate and glutamate carboxyls exhibit Raman bands characteristic of their ionized (CO_2^- symmetric stretching, *ca.* 1400–1420 cm^{-1}) and protonated forms (C=O stretching, *ca.* 1700–1750 cm^{-1}) (Fasman et al., 1978b). The pH 4.0 spectrum of Figure 3 displays a weak band near 1718 cm^{-1} which is diminished in intensity at pH 7.0, indicating titration of COOH to COO^- between pH 4.0 and pH 7.0. The higher concentration of COO^- groups at pH 7.0 is also reflected in the greater Raman intensity at *ca.* 1405–1407 cm^{-1} in the pH 7.0 spectrum. Thus, the positive difference band at 1718 cm^{-1} and the negative difference band at 1405 cm^{-1} in the pH 4.0 – pH 7.0 difference spectrum of Figure 3 demonstrate the titration of Asp and/or Glu side-chain carboxyls with increasing pH.

In Figure 3, the pH 7.9 – pH 7.0 difference spectrum reveals a *negative* difference band at *ca.* 1710 cm^{-1}, indicating that the COOH population is greater at pH 7.0 than at pH 7.9; i.e., a significant fraction of COOH groups is titrated above pH 7.0. The carboxyl group contributing to the negative difference band is most likely Asp26, which is shown to have a pK_a of 7.5 in $TRX(S)_2$ (Langsetmo et al., 1991b). The data of Figure 3 do not permit accurate determination of carboxyl pK_a values, but do show clearly that the titration is not complete at pH 7.0.

Interestingly, the pH 7.9 – pH 7.0 difference spectrum exhibits a negative difference band at 1406 cm^{-1}, showing that the higher COO^- population at pH 7.9 is offset by other factors which diminish the Raman intensity in this spectral region. This could be due to specific interactions of carboxyl groups (e.g., with positively charged groups or ions) or to other structural features which contribute Raman intensity at *ca.* 1406 cm^{-1} at pH 7.9 but not at pH 7.0.

Other Side Chains. Among the prominent features observed in the Figure 3 difference spectra (below pH 7.9) are troughs in the regions 900–950, 1060–1080, and 1474 cm^{-1}. These bands are reasonably assigned to skeletal modes (C–C, C–N, C–O stretching) of many side chains, and to methyl group deformation modes of various aliphatic side chains (Thomas et al., 1983). Although more specific assignments and detailed structural interpretations are not possible from the present data, the results indicate that titration of the active center generates environmental and possibly configurational changes in many residues. These changes occur with virtually no change in thioredoxin secondary structure, since amide I and amide III markers are not affected between pH 4.0 and pH 7.9.

The difference spectrum between pH 12.2 and pH 7.0 (Figure 3, bottom) exhibits a much larger number of difference peaks and troughs, indicative of much more extensive change in thioredoxin side-chain environments with dithiolate formation.

Secondary Structure Markers. The pH 12.2 – pH 7.0 difference spectrum of Figure 3 reveals substantial changes of secondary structure with dithiolate formation. Both amide I and amide III are broadened considerably, yet retain their peak centers in the intervals expected for β structure. This implies the presence of much β structure in the dithiolate form at pH 12.2, and is consistent with circular dichroism spectra which indicate that thioredoxin is only partially through

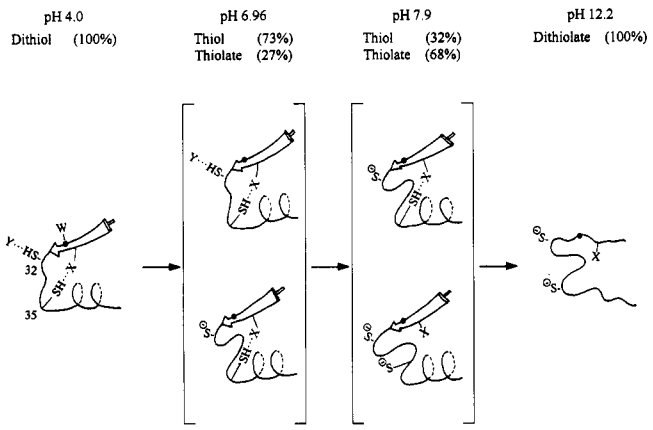

FIGURE 6: Model for titration of active-center cysteines of thioredoxin. The letters X and Y represent the acceptors of hydrogen bonds from the SH donors of Cys35 and Cys32, respectively. Candidates for X and Y are the Asp26 carboxylate C=O and a water oxygen, respectively. See text.

the unfolding transition at pH 12.2 (C. Hanson and C. Woodward, unpublished results).

CONCLUSIONS

The active-site cysteines of reduced thioredoxin are neither structurally nor chemically equivalent, and both titrate with $pK_a < 8.2$. Although both cysteines function structurally as hydrogen-bond donors, one (assigned tentatively as Cys35) donates a measurably stronger hydrogen bond than the other. The likely acceptor to the strong hydrogen-bond donor is a carbonyl oxygen. The other cysteine donor (assigned to Cys32) may hydrogen-bond to either a water oxygen or another comparable acceptor. The chemically distinct environments of Cys32 and Cys35 are manifested in their pH titrations. By decomposing the complex Raman sulfhydryl band of $TRX(SH)_2$ as a function of pH, we have determined that the thiol → thiolate equilibria are governed by $pK_{C32} = 7.1 \pm 0.2$ and $pK_{C35} = 7.9 \pm 0.2$.

The Raman spectra show that titration of the active-center cysteines induces conformational changes in the cysteinyl side chains (torsion X^1), evidenced by a decrease in trans rotamers of the Hα–Cα–Cβ–S network between pH 4.0 and pH 7.0. Additional conformational changes occur in the cysteine side chains as the pH is further increased. Simultaneously, changes occur in tryptophan (Trp28 and Trp31) side-chain conformations (torsion $X^{2,1}$), indole hydropathic environments, and hydrogen bonding of 1N–H. Protonation states and environments of side-chain carboxylate groups are also affected. Although the affected carboxylate residue(s) cannot be identified unambiguously from the present Raman data, the results are consistent with involvement of Asp26, which has been implicated in oxidoreductase activity (Langsetmo et al., 1991a).

Collectively, the present results suggest a titration scheme like that depicted in Figure 6. Specific features of this model, which can be tested by future experiments, are the following: (i) Strong hydrogen bonding occurs between the Cys35 S–H donor of $TRX(SH)_2$ and a highly electronegative acceptor (such as the C=O of Asp26). (ii) Somewhat weaker hydrogen bonding occurs for Cys32, probably involving an –O– acceptor of solvent H_2O or hydroxyl side chain. (iii) Titration of the Cys32 SH to thiolate ion is near its midpoint at pH 7, with relatively little titration of Cys35. (iv) Between pH 4.0 and pH 7.0, a population of COOH groups is titrated to CO_2^-, and the hydrophilic environments of Trp28 and Trp31 indoles are rendered slightly less hydrophilic. (v) A population of COOH groups with $pK_a > 7.0$ exists in reduced thioredoxin. (vi) At pH 7.9, Cys32 is predominantly in the thiolate form, while equal populations of thiol and thiolate forms of Cys35 coexist. (vii) At pH 4–8, the phenoxyl groups of Tyr49 and Tyr70 act, virtually exclusively, as strong hydrogen-bond donors, indicating that they are not in contact with the aqueous solvent. The fact that this hydrogen bonding is unperturbed with titration of the active center up to pH 8 indicates that the phenoxyls are not coupled structurally to the active-center thiols. Tyrosine Raman markers also preclude solvent exposure of the phenoxyls in the partially unfolded dithiolate form of thioredoxin at pH 12.2. (viii) The secondary structure of thioredoxin does not change significantly with thiol titrations between pH 4.0 and pH 7.9.

Raman amide bands of thioredoxin indicate a solution secondary structure containing substantial β-sheet, as expected from NMR and X-ray studies. The Raman amide markers confirm other reports that this secondary structure is virtually invariant to oxidation. Nevertheless, $TRX(SH)_2$ and $TRX(S)_2$ exhibit pronounced differences in Raman bands assigned to various side chains (Table I and Figure 2), indicating that the solution structures of $TRX(SH)_2$ and $TRX(S)_2$ differ with respect to the environments and interactions of these side-chain groups. This could arise from differences at the interfaces between elements of secondary structure in reduced and oxidized forms, with relatively little difference in the respective main-chain conformations.

The present study demonstrates the suitability of Raman spectroscopy for determining pK_a values governing thiol → thiolate equilibria. In proteins containing a single cysteine, the pK_a may be determined directly by measuring the appropriately normalized SH Raman band intensity as a function of pH. For this purpose, the Raman band of *in situ* N_2 is most conveniently exploited as the internal normalization standard (Li et al., 1993). In proteins containing more than a single sulfhydryl, an average pK_a may also be calculated directly from measurements of the complex SH band intensity. If the constituent cysteines exist in sufficiently different environments, as is the case here for *E. coli* thioredoxin, the individual pK_a values can be computed by appropriate resolution of the individual band components. In future work, the method developed here will be applied to mutant thioredoxins to further elucidate coupled conformational changes at the active center. Similar approaches will be pursued in the study of glutaredoxin and other redox-active cysteinyl proteins.

ACKNOWLEDGMENT

We thank Ms. Kelly Aubrey-Robertson for assistance with preparation of the figures.

REFERENCES

Chen, M. C., & Lord, R. C. (1974) *J. Am. Chem. Soc. 96*, 4750–4752.
Dyson, J. H., Gippert, G. P., Case, D. A., Holmgren, A., & Wright, P. E. (1990) *Biochemistry 29*, 4129–4136.
Dyson, J. H., Tennant, L. T., & Holmgren, A. (1991) *Biochemistry 30*, 4262–4268.
Fasman, G. D., Itoh, K., Liu, C. S., & Lord, R. C. (1978) *Biopolymers 17*, 1729–1746.
Forman-Kay, J. D., Clore, M., & Gronenborn, A. M. (1992) *Biochemistry 31*, 3442–3452.
Gleason, F. K. (1992) *Protein Sci. 1*, 609–616.
Harada, I., Miura, T., & Takeuchi, H. (1986) *Spectrochim. Acta 42A*, 307–312.

Herzberg, G. (1950) *Molecular Spectra and Molecular Structure I. Spectra of Diatomic Molecules*, 2nd ed., D. Van Nostrand, Princeton, NJ.
Holmgren, A. (1985) *Annu. Rev. Biochem. 54*, 237–271.
Holmgren, A. (1989) *J. Biol. Chem. 264*, 13963–13966.
Kallis, G. B., & Holmgren, A. (1980) *J. Biol. Chem. 255*, 10261–10265.
Kaminsky, S. M., & Richards, F. M. (1992a) *Protein Sci. 1*, 10–21.
Kaminsky, S. M., & Richards, F. M. (1992b) *Protein Sci. 1*, 22–30.
Katti, S. K., LeMaster, D. M., & Eklund, H. E. (1990) *J. Mol. Biol. 212*, 167–184.
Kitagawa, T., Azuma, T., & Hamaguchi, K. (1979) *Biopolymers 18*, 451–465.
Langsetmo, K., Fuchs, J. A., & Woodward, C. (1989) *Biochemistry 28*, 3211–3220.
Langsetmo, K., Fuchs, J. A., & Woodward, C. (1991a) *Biochemistry 30*, 7603–7609.
Langsetmo, K., Fuchs, J. A., Woodward, C., & Sharp, K. A. (1991b) *Biochemistry 30*, 7609–7614.
Laurent, T. C., Moore, E. C., & Reichard, P. (1964) *J. Biol. Chem. 239*, 3436–3444.
Li, H., & Thomas, G. J., Jr. (1991) *J. Am. Chem. Soc. 113*, 456–462.
Li, H., Wurrey, C. J., & Thomas, G. J., Jr. (1992) *J. Am. Chem. Soc. 114*, 7463–7469.
Li, H., Tuma, R., Vohnik, S., & Thomas, G. J., Jr. (1993) (submitted for publication).
Li, T., Chen, Z., Johnson, J. E., & Thomas, G. J., Jr. (1992) *Biochemistry 31*, 6673–6682.
Lord, R. C., & Yu, N.-T. (1970) *J. Mol. Biol. 50*, 509–524.
Lundstrom, J., Krause, G., & Holmgren, A. (1992) *J. Biol. Chem. 267*, 9047–9052.
Merola, F., Rigler, R., Holmgren, A., & Brochon, J.-C. (1989) *Biochemistry 28*, 3383–3398.
Miura, T., Takeuchi, H., & Harada, I. (1989) *J. Raman Spectrosc. 20*, 667–671.
Miura, T., Takeuchi, H., & Harada, I. (1991) *Biochemistry 30*, 6074–6080.
Nogami, N., Sugeta, H., & Miyazawa, T. (1975a) *Chem. Lett. (Jpn.)*, 147–150.
Nogami, N., Sugeta, H., & Miyazawa, T. (1975b) *Bull. Chem Soc. Jpn. 48*, 2417–2420.
Ozaki, Y., Sugeta, H., & Miyazawa, T. (1975) *Chem. Lett. (Jpn.)*, 713–716.
Rava, R. P., & Spiro, T. G. (1985) *J. Am. Chem. Soc. 24*, 1861–1865.
Reutimann, H., Straub, B., Luisi, P.-L., & Holmgren, A. (1981) *J. Biol. Chem. 256*, 6796–6803.
Russel, M. (1991) *Mol. Microbiol. 5*, 1607–1613.
Siamwiza, M. N., Lord, R. C., Chen, M. C., Takamatsu, T., Harada, I., Matsuura, H., & Shimanouchi, T. (1975) *Biochemistry 14*, 4870–4876.
Sugeta, H., Go, A., & Miyazawa, T. (1972) *Chem. Lett. (Jpn.)*, 83–86.
Sugeta, H., Go, A., & Miyazawa, T. (1973) *Bull. Chem. Soc. Jpn. 46*, 3407–3411.
Thomas, G. J., Jr., & Barylski, J. (1970) *Appl. Spectrosc. 24*, 463–464.
Thomas, G. J., Jr., & Agard, D. A. (1984) *Biophys. J. 46*, 763–768.
Thomas, G. J., Jr., Prescott, B., & Day, L. A. (1983) *J. Mol. Biol. 165*, 321–356.
Thomas, G. J., Jr., Prescott, B., Benevides, J. M., & Weiss, M. A. (1986) *Biochemistry 25*, 6768–6778.
Thomas, G. J., Jr., Prescott, B., & Urry, D. W. (1987) *Biopolymers 26*, 921–934.
Yu, T.-J., Lippert, J. L., & Peticolas, W. L. (1973) *Biopolymers 12*, 2161–2176.
Van Wart, H. E., & Scheraga, H. A. (1986) *Proc. Natl. Acad. Sci. U.S.A. 83*, 3064–3067.
Verduin, B. J. M., Prescott, B., & Thomas, G. J., Jr. (1984) *Biochemistry 23*, 4301–4308.